OPEN ACCESS Freely available online

Biochemistry & Pharmacology: Open Access

Research Article

Sex-specific Gene Expression in Flupirtine-Treated *Cln3*$^{\Delta ex7/8}$ Mouse Brain

Joelle Makoukji[1], Sara Saab[1], Katia Maalouf[1], Nadine J. Makhoul[1], Angelica V. Carmona[2], Nihar Kinarivala[3], Paul C. Trippier[2,4,5], Rose-Mary Boustany[1,6*]

[1]*Department of Biochemistry and Molecular Genetics, American University of Beirut Medical Center, Beirut, Lebanon;*

[2]*Department of Pharmaceutical Sciences, University of Nebraska Medical Center, Omaha, USA;*

[3]*Department of Pharmaceutical Sciences, Jerry H. Hodge School of Pharmacy, Texas Tech University Health Sciences Center, Amarillo, USA*

[4]*Department of Oncology, University of Nebraska Medical Center, Omaha, USA;*

[5]*Department of Pharmaceutical Sciences, University of Nebraska Medical Center, Omaha, USA;*

[6]*Department of Pediatrics and Adolescent Medicine, American University of Beirut Medical Center, Beirut, Lebanon*

ABSTRACT

Gene expression is a powerful tool to understand structure-function relationships in the nervous system. This study reports global gene expression changes induced by flupirtine in brain of male and female *Cln3*$^{\Delta ex7/8}$ mice, exposing potential flupirtine targets at the molecular level. Gene expression analysis of male and female *Cln3*$^{\Delta ex7/8}$ mouse brain was determined following oral administration of flupirtine for 14 weeks, using Mouse Genome 430 2.0 array Chips and an Affymetrix platform. Fifty-six genes in males and 79 in females were differentially expressed in flupirtine- versus vehicle-treated *Cln3*$^{\Delta ex7/8}$ mouse brain. Flupirtine altered several pathways in *Cln3*$^{\Delta ex7/8}$ mouse brain: apoptosis, the complement cascade, NF-kB, and p38α MAPK signaling pathways. Gene-gene network analysis highlighted networks and processes functionally pertinent to flupirtine treatment. These encompassed neurodegeneration, neuro-inflammation, and implicated neurological disorders such as Alzheimer and Parkinson disease. Flupirtine mediates its action in males and females through distinctive actionable targets in the same pathways. This work consolidates the groundwork for considering flupirtine as a treatment option in human CLN3 disease.

Keywords: Neurodegeneration; Neuronal ceroid lipofuscinoses; CLN3 disease; Flupirtine; Gene expression; p38 MAPK signaling pathway

INTRODUCTION

Juvenile Neuronal Ceroid Lipofuscinosis (JNCL), now known as CLN3 disease, is a fatal inherited neurodegenerative disorder affecting children. It leads to death in the second decade of life. CLN3 disease is the most common of a number of disorders grouped as the Neuronal Ceroid Lipofuscinoses (NCLs). This childhood disorder results in visual failure, seizures, cognitive and motor decline [1]. Pathological hallmarks of CLN3 disease include accelerated neuronal apoptosis, accumulated autofluorescent material in neurons, and increased ceramide levels in brain and serum of patients [2,3]. Present treatment for this disease is symptomatic, highlighting the importance of identifying pathology-modifying drugs. The non-opioid analgesic drug, flupirtine, confers neuroprotection to CLN3-deficient cell lines [4], and Cln3$^{\Delta ex7/8}$ knock-in mice [5]. The Cln3$^{\Delta ex7/8}$ knock-in mouse harbors the common human 1.02 kb deletion that eliminates exons 7/8 of the Cln3 gene, and recapitulates

Correspondence to: Rose-Mary Boustany, Department of Pediatrics and Adolescent Medicine, American University of Beirut Medical Center, Beirut, Lebanon, Tel: 961 350 000; E-mail: rb50@aub.edu.lb

Received: February 12, 2021; **Accepted:** February 26, 2021; **Published:** March 05, 2021

Citation: Joelle Makoukji, Saab S, Maalouf K, Makhoul NJ, Carmona AV, Boustany RM, et al. (2021) Sex-Specific Gene Expression in Flupirtine-Treated *Cln3*$^{\delta ex7/8}$ Mouse Brain. Biochem Pharmacol 10.272

neuropathological, behavioral, and biochemical changes seen in human CLN3 disease [6].

Flupirtine is a centrally acting, non-opioid analgesic drug belonging to the triaminopyrimidines [7]. Flupirtine maleate is the salt of this drug, hereafter referred to as flupirtine. It is an effective analgesic [7,8] additionally providing neuroprotective, muscle relaxant, and antiepileptic properties, key pathological and clinical features of the NCLs [9]. Flupirtine treatment blocks apoptosis in neurons from chronically stressed mice [10]. There is evidence that suggests that flupirtine reduces brain injury, induces remodeling of brain tissue, and cognitive impairment in vivo animal models of ischemic stroke [7]. Knocking down CLN3 protein expression enhances apoptosis rates. Flupirtine treatment blocks apoptosis in CLN1-, CLN2-, CLN3 and CLN6-deficient cells post-etoposide treatment [11]. Pretreating hNT human neuronal cells with flupirtine successfully prevents apoptosis [11]. Flupirtine protects PC12 neuronal precursor cells against etoposide induced cell death by rescuing them from apoptosis [4,12], and, also imparts neuroprotection to human post-mitotic hNT neurons [11]. Flupirtine protects neuronal post-mitotic hNT cells from death by increasing expression of Bcl-2 protein, a potent anti-apoptotic agent [11] and is neuroprotective in etoposide-treated human SH-SY5Y neuroblastoma cells [12]. Its neuroprotective effects are confirmed in human induced pluripotent stem cells, iPSC-derived neurons and CLN3-deficient lymphoblasts [12]. Flupirtine positively modulates cell growth and reduces apoptosis in CLN3-deficient PC12 cells [4]. Flupirtine elevates BCL-2 mRNA expression in CLN3-deficient PC12 cells, and downregulation of Caspase 3 and 8 levels, all contributing to diminished apoptosis [4].

Oral supplementation of homozygous *Cln3*$^{\Delta ex7/8}$ mice with flupirtine for a period of 14 weeks results in significant improvement in the course of CLN3 disease with improvement of neurobehavioral parameters, reduced astrogliosis and increased neuronal cell counts in specific brain regions in male and female *Cln3*$^{\Delta ex7/8}$ mice [5]. Identification of altered gene expression in response to drugs can provide insight into pathogenic mechanisms. Brain transcriptome description provides insight into drug-specific molecular mechanisms. We previously identified gender-specific genes involved in neuroprotective mechanisms of galactosylceramide in CLN3 disease in brains of male and female *Cln3*$^{\Delta ex7/8}$ mice [13]. Sex differences in mitochondrial brain pathology and onset in the Alzheimer 3xTg mouse model have been confirmed as earlier and more severe in females and addressed as a necessary prerequisite to evaluate potential therapies for neurodegenerative diseases [14]. To explore changes in gene patterns preceding neuroprotection conferred by flupirtine in CLN3 disease, and to compare expression of ≈ 45,000 transcripts in brain of *Cln3Δex7/8* male and female mice treated with flupirtine or vehicle, Affymetrix mRNA chips were used. Analysis reveals statistically significant differences in gene expression and pathways including the MAPK signaling pathway. This may in part explain the positive therapeutic effects observed in flupirtine-treated *Cln3*$^{\Delta ex7/8}$ mice. We uncovered that flupirtine mediates its action in males and females via distinctive actionable targets in the same pathway, ascertaining gender dimorphism response to flupirtine. This data set provides an important illustration of flupirtine targets at the molecular level that result in rescuing homozygous *Cln3*$^{\Delta ex7/8}$ mouse brain from neurodegenerative processes due to lack of functional CLN3 protein. This work solidifies the premise for using flupirtine in the treatment of human CLN3 disease in both males and females.

MATERIALS AND METHODS

Animal housing

Mouse work was in accordance with American University of Beirut (AUB) Institutional Animal Care and Use Committee (IACUC) guidelines (IACUC approval number: 18-08-496). Mouse testing occurred at the AUB Animal Care Facility. C57BL/6J and homozygous *Cln3*

mice (Jackson laboratory) were kept in a 12-hour light/dark cycle and supplied with ad libitum access to food and water. Room temperature was maintained at 19-22°C, and relative humidity at 30-50%. Mice are housed three-four/cage. All efforts to minimize number of mice and suffering are applied. Mice are bred in-house to obtain the number needed (n=24), and monitored for weekly weight, basic behavior and general health throughout the study. All treated mouse groups were indistinguishable from non-treated WT controls with respect to body weight and fur, indicating lack of adverse effects. Prior to treatment, at age four weeks (weaning), tail tips were used for DNA extraction and genotyping by polymerase chain reaction (PCR). Mice are divided into three groups: vehicle-treated WT mice, vehicle-treated *Cln3*$^{\Delta ex7/8}$ mice, and flupirtine-treated *Cln3*$^{\Delta ex7/8}$ mice. Each group consists of eight mice (four males and four females).

Flupirtine treatment

The drug in this study is flupirtine maleate, hereafter referred to as flupirtine. Flupirtine is dissolved in 0.5% di-Methyl Sulfoxide (DMSO) and in 10% phosphate-buffered saline (PBS) at a dose of 30 mg/kg body weight and given orally for a period of 14 weeks starting at age four weeks as previously described in the literature. Vehicle treatment consisted of 0.5% DMSO in 10% of PBS supplied with drinking water. Vehicle and flupirtine are administered in drinking water in a volume of ≈ eight ml/day/mouse 'per os'. Flupirtine production occurred in Dr. Paul Trippier laboratory while he was still at Texas Tech University Health Sciences Center, Department of Pharmaceutical Sciences, and School of Pharmacy.

RNA extraction from mouse brain tissue

Eighteen week-old vehicle-treated WT (n=4), vehicle-treated *Cln3*$^{\Delta ex7/8}$ (n=4), and flupirtine-treated *Cln3*$^{\Delta ex7/8}$ (n=4) male and female mice were deeply anesthetized with a mixture of Xylazine and Ketamine (10 mg/kg and 100 mg/kg, respectively) and brains rapidly dissected and "snap" frozen in liquid nitrogen,

prior to storage at -80°C for later use. Brain tissues were ground and 30 mg of ground tissue were used to isolate total RNA using RNeasy Plus Mini Kit (Cat No. 74134, Qiagen, USA) according to manufacturer protocols.

RNA integrity was assessed using the ExperionTM Automated Electrophoresis System (BioRad, CA, USA). RNA concentrations were determined by absorption at 260 nm wavelength and RNA purity was checked with A260/A280 and A260/A230 ratios (Nanodrop-DeNovix DS-11FX Spectrophotometer, DE, USA).

Microarray gene expression profiling

Microarray technology was employed to define unique and common gene expression profiles and pathways involved in mouse brains. Brain RNA from 23 mice were used for gene expression data analysis (Males: 3 vehicle-treated WT, 4 vehicle-treated *Cln3*$^{\Delta ex7/8}$ and 4 flupirtine-treated *Cln3*$^{\Delta ex7/8}$; Females: 4 vehicle-treated WT, 4 vehicle-treated *Cln3*$^{\Delta ex7/8}$ and 4 flupirtine-treated *Cln3*$^{\Delta ex7/8}$). Males and females were analyzed separately. Analysis was conducted using the GeneChip® Mouse Genome 430 2.0 array (Affymetrix Inc., CA, USA) which encompasses 45,000 probe sets. Samples were prepared and microarrays processed using the GeneChipTM 3' IVT PLUS Reagent Kit (Thermo Fisher Scientific, MA, USA) according to manufacturer instructions. Briefly, 100 ng of total brain RNA were labeled, fragmented, then hybridized to arrays. This was followed by washing and staining using the GeneChip Fluidics Station 450 (Thermo Fisher Scientific, MA, USA). Next, arrays were scanned using the GeneChip Scanner 3000 7G (Thermo Fisher Scientific, MA, USA). Cell Intensity Data (CEL) files were generated using the Affymetrix GeneChipTM Command Console (AGCC) software version 3.2 (Thermo Fisher Scientific, MA, USA).

Data analysis

Data analysis used Partek® Genomics Suite® software (version 7.0, Partek, MO, USA). Stringent quality control criteria were applied to raw data. Probe set data were summarized and background adjusted using the Robust Multi-Array Average (RMA) algorithm. Raw data is normalized through non-linear transformation termed Quantile Normalization and then filtered to remove noise and extreme expression values. False discovery rate (FDR) was not applied to the microarray data after statistical testing as there were no genes that met a FDR p-value<0.05 for flupirtine treatment effect in either gender. To overcome this issue, dysregulated genes identified by microarray analysis were evaluated by quantitative real-time transcription polymerase chain reaction (qRT-PCR). In this case, it is acceptable not to apply FDR correction, allowing examination of a larger pool of differentially expressed genes.

Two-way variance (ANOVA) analysis to detect differences of groups with gender as a variable is used. Treatment and no treatment constitute the basis for comparing different groups. All further sub-lists were created using genes that passed ANOVA p-value and fold-change thresholds (p-value<0.05 considered significant; arbitrary threshold of 1.3-fold difference used to discern differentially modulated genes). Clustering and gene ontology (GO) analyses were performed (Partek Genomics Suite and Partek PathwayTM version 7.0, Partek, MO, USA) and networks of biologically related genes depicted (Pathway Studio version 11.4, Ariadne Genomics, USA).

Quantitative real-time polymerase chain reaction (qRT-PCR)

Validation of microarray results was achieved by quantitative real-time PCR (qRT-PCR). Total RNA mouse brain samples were reverse-transcribed to cDNA (QuantiTect Reverse Transcription Kit, Cat No. 205311, Qiagen, USA) according to manufacturer guidelines. qRT-PCR reactions took place using 384-well plates and specific primers at a Tm=60°C (Macrogen, South Korea). Amplification was achieved using the iQTM SYBR® Green Supermix (BioRad, CA, USA) and a CFX384TM Real-Time PCR machine. To characterize generated amplicons and to control contamination by unspecific by-products, melt curve analysis was applied. β-actin or Gapdh were used for normalization. All reactions were performed in duplicate and results were calculated using the ΔΔCt method. For sequences of primers see Table S1.

Statistical analysis

Continuous data depiction is as mean ± standard error of the mean (SEM). For two group comparison, Student's t-test is used with quantitative continuous variables. Comparisons between groups are statistically tested with one-way analysis of variants (ANOVA) followed by Tukey's post-hoc test for multiple group comparisons. Statistical significance is assumed at a p-value level of 0.05 (GraphPad Prism 6, CA, USA). Affymetrix expression data was analyzed using Partek Genomics Suite and Partek Pathway™ version 7.0 (Partek, MO, USA). All tests were two sided and a p-value<0.05 was considered statistically significant (*p<0.05, **p<0.01, ***p<0.001, ****p<0.0001).

RESULTS AND DISCUSSION

Transcriptional profiles of flupirtine-treated male and female *Cln3*$^{\Delta ex7/8}$ brain tissue

Gene expression profiling of brain tissue of *Cln3*$^{\Delta ex7/8}$ mice treated with flupirtine or vehicle were compared (Affymetrix Mouse Genome platform). Differentially expressed genes (DEGs) in brain from flupirtine and vehicle-treated *Cln3*$^{\Delta ex7/8}$ mice were identified. Genes were considered statistically significantly at a p-value<0.05 and exceeded an arbitrary fold change of ≥ ± 1.3. In a probe-level analysis, using two-way ANOVA, male mice had 56 DEGs (46 downregulated and 10 upregulated genes) modulated in brain tissue from flupirtine-treated mice compared to vehicle-treated male mice. In female mice, 79 genes are differentially modulated in flupirtine treatment versus vehicle treatment groups, 36 of which were downregulated and 43 genes up-

regulated by flupirtine and these differences were statistically significant (Figure 1). DEGs for males and females are listed in supplementary. Figure 2 shows the hierarchical clustering (2D-heatmap) of significantly modulated genes in male (Figure 2A) and female (Figure 2B) *Cln3*$^{\Delta ex7/8}$ mouse brains.

Major pathways modulated by flupirtine in male and female *Cln3*$^{\Delta ex7/8}$ brain

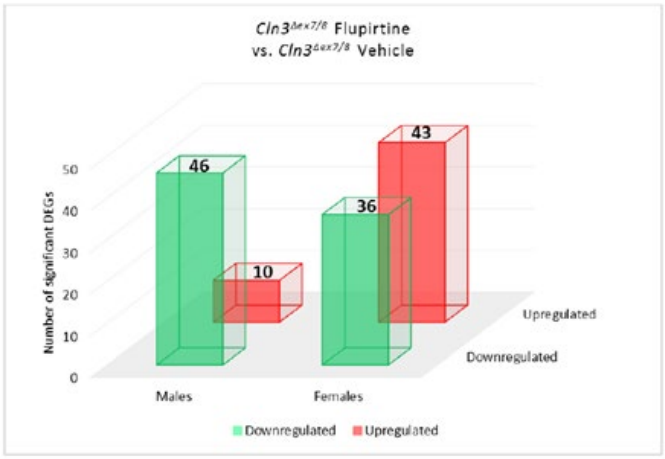

Figure 1: Flupirtine induces sex-specific alterations of gene expression in *Cln3*$^{\Delta ex7/8}$ mouse brain. Bar chart indicating numbers of significantly and differentially expressed genes impacted by flupirtine versus vehicle in *Cln3*$^{\Delta ex7/8}$ male and female mice. A cut-off p-value < 0.05 and fold-change ≥ ±1.3 were assumed to uncover genes significantly modulated by flupirtine compared to vehicle.

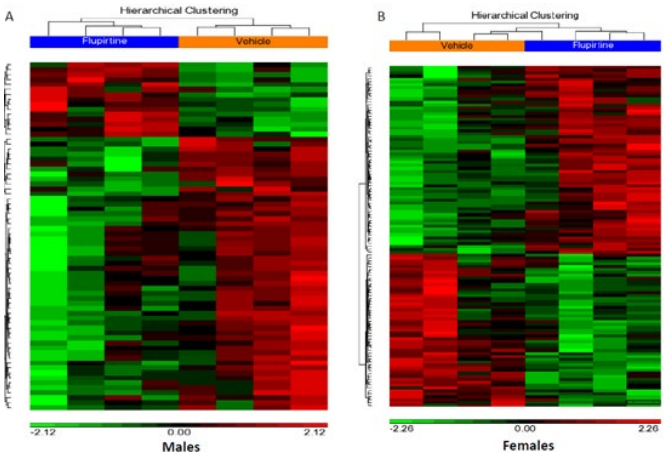

Figure 2: Differentially expressed genes in brain of flupirtine- versus vehicle-treated male and female *Cln3*$^{\Delta ex7/8}$ mice. Two-dimensional heat maps of (A) 56 DEGs in male and (B) 79 DEGs in female *Cln3*$^{\Delta ex7/8}$ mouse brain. Heat maps depict mRNA abundance intensities of differentially expressed genes in profiled samples. Robust Multi-Array Average (RMA) preprocessed data is transformed to z-scores. The legend represents relative over- and under-expression in red and green, respectively. Labeling at the top represents vehicle versus flupirtine-treated samples. A cut-off p-value < 0.05 and fold-change ≥ ±1.3 were assumed to identify genes significantly modulated by flupirtine treatment.

To dissect the molecular pathways affected by flupirtine treatment further, Kyoto Encyclopedia of Genes and Genomes (KEGG) Pathway database in Partek Pathway was used. Relevant candidate pathways related to apoptosis and modulated by flupirtine treatment are the "MAPK signaling pathway" and "cellular senescence". All significantly enriched canonical pathways in *Cln3*$^{\Delta ex7/8}$ male mouse brain are represented. An upregulated gene involved in these pathways is Dusp1 (Table S2). Downregulated genes comprised Tgfβr1, Ppp3r1, C1qb, and Pi3k/Akt (Table S3). In female *Cln3*$^{\Delta ex7/8}$ mouse brain, functionally important pathways included "apoptosis pathway", "longevity regulating pathway", and "p53 signaling pathway". All significantly enriched canonical pathways in Cln3$^{\Delta ex7/8}$ female mouse brains. Some of the upregulated genes involved in these pathways are Ppm1d, Xpa, Xiap, and Ccne2 (Table S4). Downregulated genes that are modulated by aforementioned pathways include Pi3k/Akt, Rapgef4, Map3k14, C1ra, and C1rb (Table S5). Findings suggest that flupirtine leads to modulation of gene expression in *Cln3*$^{\Delta ex7/8}$ mouse brain via regulation of major metabolic and signaling pathways in males and females.

DEGs are topologically organized into functional gene-gene interaction network maps depicting contribution to different diseases in male (Figure 3) and female (Figure 4) *Cln3*$^{\Delta ex7/8}$ mice. In male *Cln3*$^{\Delta ex7/8}$ mice, flupirtine treatment implicated neurodegeneration, neuroinflammation, Alzheimer disease, toxicity and infection (Figure. 3). In brain of female *Cln3*$^{\Delta ex7/8}$ mice, diseases included neurodegeneration, neurodevelopmental disorders, Alzheimer and Parkinson disease, toxicity, traumatic brain injury, inflammation, cognitive decline, and cerebrovascular ischemia (Figure 4).

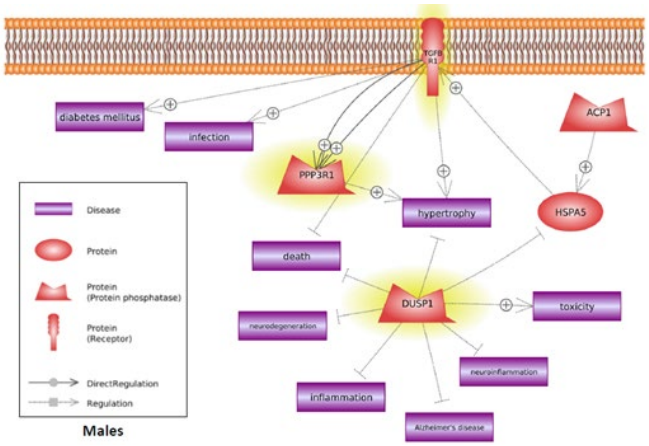

Figure 3: Gene/disease networks of significant DEGs in brain from flupirtine- versus vehicle-treated male *Cln3*$^{\Delta ex7/8}$ mice. Pathway Studio software generated network interactions between diseases and most significant DEGs in male *Cln3*$^{\Delta ex7/8}$ mouse brain (p-value < 0.05; stringency ≥ ± 1.3 fold-change in gene expression). Depiction of genes is by gene symbols. Genes involved in the most relevant pathways are highlighted with a yellow halo. Indirect (dotted gray lines), direct regulation (full black lines), expression (blue lines) and binding (purple lines).

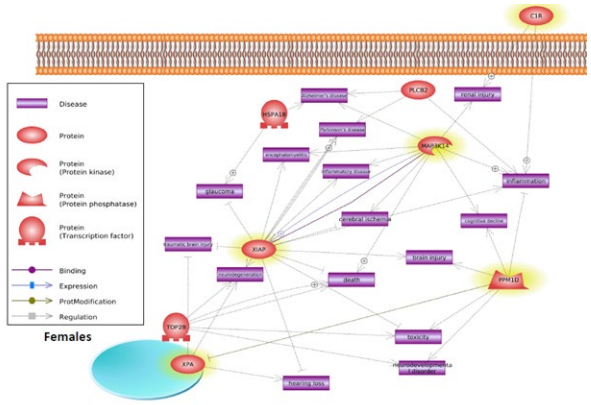

Figure 4: Gene/disease networks of significant DEGs in brain from flupirtine- versus vehicle-treated female *Cln3*$^{\Delta ex7/8}$ mice. Pathway Studio software generated network interactions between diseases and most significant DEGs in female *Cln3*$^{\Delta ex7/8}$ mouse brain (p-value < 0.05; stringency ≥ ± 1.3 fold-change in gene expression). Depiction of genes is by gene symbols. Genes involved in the most relevant pathways are highlighted with a yellow halo. Indirect (dotted gray lines), direct regulation (full black lines), expression (blue lines) and binding (purple lines).

Validation of mRNA microarray results by qRT-PCR

Six modulated genes were chosen at random underwent analysis. qRT-PCR is the gold standard to validate dysregulated gene expression results. Flupirtine induces significant downregulation in expression of Nostrin (p-value<0.01), Pi3k/Akt (p-value<0.05) and a significant upregulation of Dusp1 (p-value<0.05) in male Cln3Δex7/8 mice compared to vehicle-treated *Cln3*$^{\Delta ex7/8}$ mice (Figures 5). Findings by qRT-PCR correlated with microarray analysis, validating results. In females, key DEGs expression is validated by qRT-PCR and follows a similar trend. Flupirtine-treated female *Cln3*$^{\Delta ex7/8}$ mice show significant upregulation of Ppm1d (p-value<0.05), Xiap (p-value<0.05) and significant downregulation in C1ra (p-value<0.05) expression in comparison with vehicle-treated Cln3Δex7/8 mice (Figures 6).

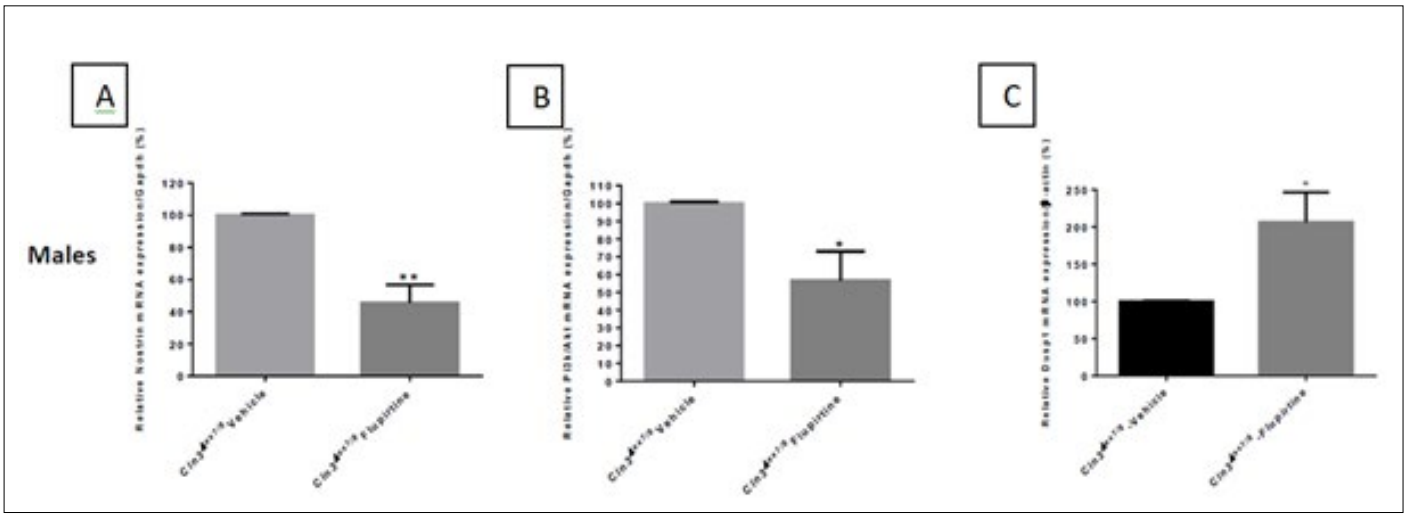

Figure 5: Validation of microarray results with qRT-PCR in brain from male *Cln3*$^{\Delta ex7/8}$ mice. Relative mRNA expression measured by qRT-PCR. The following differentially expressed genes in male *Cln3*$^{\Delta ex7/8}$ mouse brains were randomly chosen from statistically significant dysregulated genes: (A) Nostrin, (B) Pi3k/Akt, and (C) Dusp1. Values are means of the fold changes normalized to β-actin or Gapdh mRNA expression with standard errors represented by vertical bars. *p-value < 0.05 and ** p-value < 0.01 by Student's t-test (n=4).

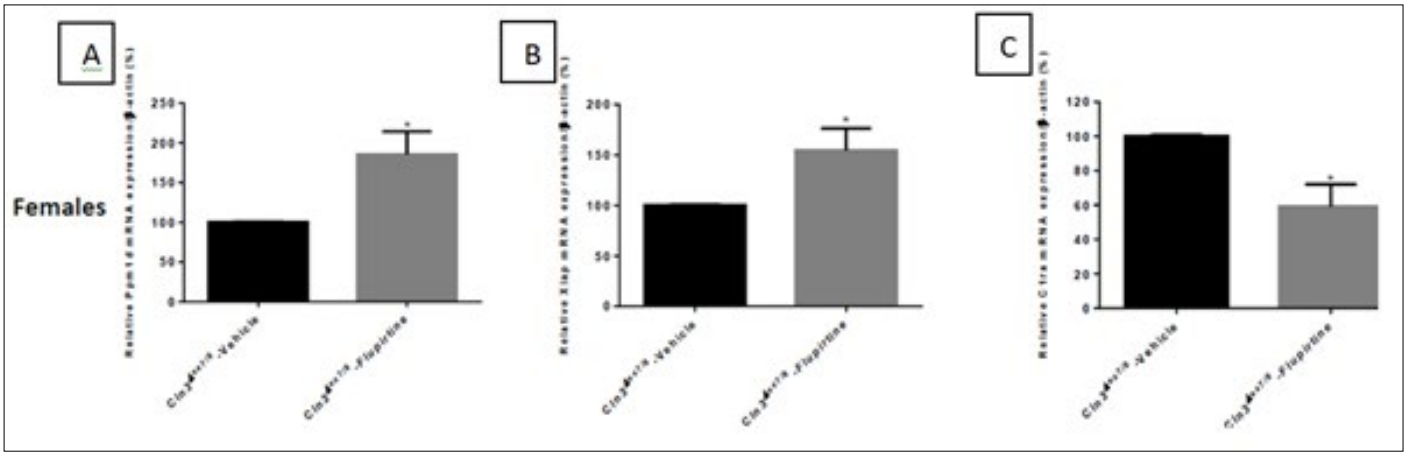

Figure 6: Validation of microarray results with qRT-PCR in brain from female *Cln3*$^{\Delta ex7/8}$ mice. Relative mRNA expression measured by qRT-PCR. The following differentially expressed genes in female *Cln3*$^{\Delta ex7/8}$ mouse brains were randomly chosen from statistically significant dysregulated genes: (D) Ppm1d, (E) Xiap, and (F) C1ra. Values are means of the fold changes normalized to β-actin or Gapdh mRNA expression with standard errors represented by vertical bars. *p-value < 0.05 and ** p-value < 0.01 by Student's t-test (n=4).

Flupirtine treatment modulates complement cascade in male and female Cln3Δex7/8 brain

Microarray analysis showed a 1.473-fold increase in expression of C1qb in brain of male vehicle-treated *Cln3*$^{\Delta ex7/8}$ versus WT mice and a 1.344-fold increase in expression of C1ra in female vehicle-treated *Cln3*$^{\Delta ex7/8}$ versus WT mouse brain (Table 1). This upregulation of C1ra expression in female vehicle-treated Cln3Δex7/8 versus WT female mouse brain was significantly validated by qRT-PCR (Figure 7). Flupirtine treatment significantly lowered gene expression of C1qb and C1ra by 1.3 fold in male and female *Cln3*$^{\Delta ex7/8}$ mice, respectively (Table 1). The results were confirmed by qRT-PCR. Although not statistically significant, there was a trend of flupirtine lowering expression of C1qb in *Cln3*$^{\Delta ex7/8}$ male mouse brain (Figure 7A). In female mice, qRT-PCR showed a significant decrease in C1ra expression in flupirtine-treated *Cln3*$^{\Delta ex7/8}$ versus vehicle-treated *Cln3*$^{\Delta ex7/8}$ female mice (Figure 7B).

Flupirtine treatment modulates NF-kB signaling pathway in male and female *Cln3*$^{\Delta ex7/8}$ brain

Microarray results showed that Xiap was upregulated in both male and female *Cln3*$^{\Delta ex7/8}$ mice treated with flupirtine compared to vehicle-treated *Cln3*$^{\Delta ex7/8}$ mice (Table 2) (Figures 8D and 8D). Upstream modulators of XIAP, however, differed between the two sexes. Flupirtine-treated male *Cln3*

mice showed significantly lower mRNA levels of Nostrin (1.461-fold) compared to male vehicle-treated *Cln3*$^{\Delta ex7/8}$ mice (Table 2). Flupirtine-treated female *Cln3*$^{\Delta ex7/8}$ mice showed less mRNA levels of Map3k14 (1.319-fold) compared to female vehicle-treated *Cln3*$^{\Delta ex7/8}$ mice (Table 2). Results were validated by qRT-PCR (Figures 8A and 8C).

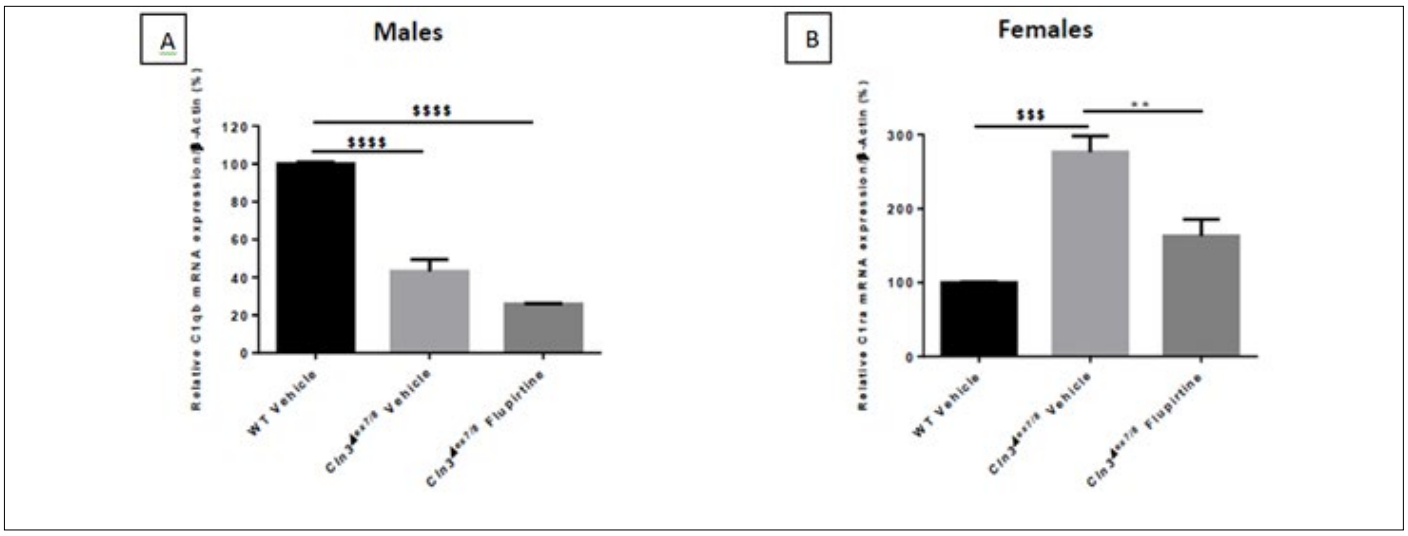

Figure 7: Relative C1qb mRNA expression measured by qRT-PCR in WT vehicle-treated, *Cln3Δex7/8* vehicle-treated and *Cln3Δex7/8* flupirtine-treated male mice. (C) Relative C1ra mRNA expression measured by qRT-PCR in WT vehicle-treated, *Cln3Δex7/8* vehicle-treated and *Cln3Δex7/8* flupirtine-treated female mice. Data are expressed as mean ± SEM. $p < 0.05 compared to vehicle-treated WT, *p <

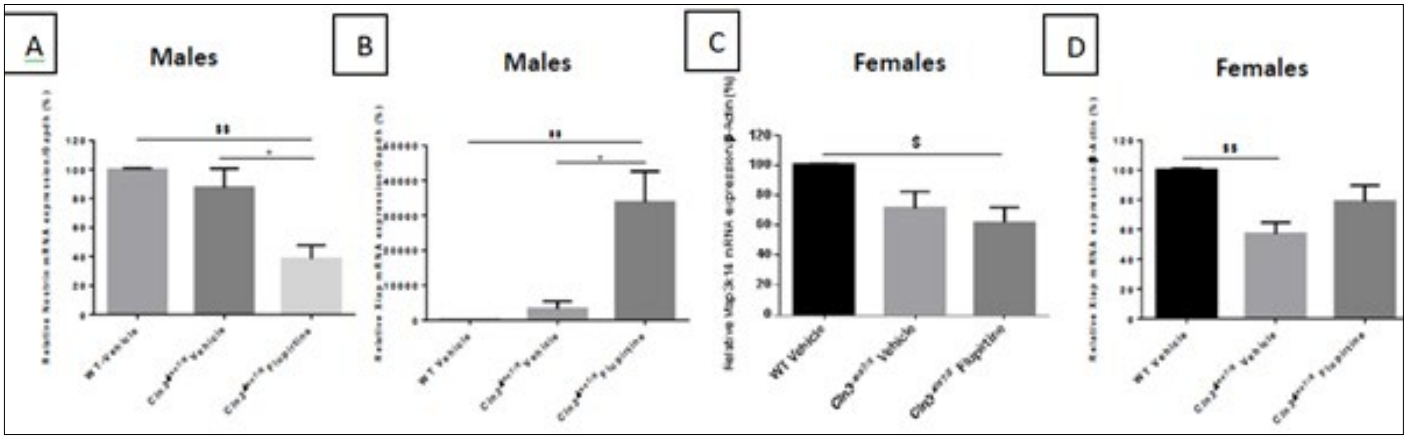

Figure 8: Relative Nostrin (A) and Xiap (B) mRNA expression measured by qRT-PCR in WT vehicle-treated, Cln3Δex7/8 vehicle-treated and *Cln3Δex7/8* flupirtine-treated male mice. Relative Map3k14 (C) and Xiap (D) mRNA expression measured by qRT-PCR in WT vehicle-treated, *Cln3Δex7/8* vehicle-treated and *Cln3Δex7/8* flupirtine-treated female mice. Data is expressed as mean ± SEM. $p < 0.05 compared to vehicle-treated WT, *p < 0.05 compared to vehicle-treated *Cln3Δex7/8* (*p < 0.05 and **p < 0.01).

Table 2: Comparative analysis of DEGs related to the NF-κB signaling pathway in brain from male and female *Cln3Δex7/8* mice. Depiction of DEGs related to the NF-κB signaling pathway in brain from male and female *Cln3Δex7/8* mice based on gene expression in flupirtine- versus vehicle-treated *Cln3Δex7/8* mice. Criteria for differential expression are a p-value < 0.05 and a stringency ≥ ± 1.3-fold change in gene expression.

Vehicle			*Cln3Δex7/8* Flupirtine vs. *Cln3Δex7/8* Vehicle		Cln3Δex7/8 Vehicle vs. WT Vehicle	
Sex	**Gene Symbol**	**Gene Title**	**p-value**	**Fold-Change**	**p-value**	**Fold-Change**
Males	Nostrin	nitric oxide synthase trafficker	0.0004	-1.461	0.227	1.25
Females	Map3k14	mitogen-activated protein kinase kinase kinase 14	0.001	-1.319	0.199	-1.157
Males	Xiap	X-linked inhibitor of apoptosis	0.396	1.046	0.048	4.015
Females	Xiap	X-linked inhibitor of apoptosis	0.019	1.335	0.075	3.125

Flupirtine treatment modulates p38/MAPK signaling pathway in male and female Cln3Δex7/8 brain

Microarray analysis and qRT-PCR revealed that Dusp1 in males and Ppm1d in females were significantly downregulated in *Cln3*$^{\Delta ex7/8}$ vehicle-treated mouse brain compared to WT (Table 3) (Figures 9A and 9B). Reduced expression of Dusp1 and Ppm1d was significantly reversed with flupirtine in diseased mice (Table 3) (Figures 9A and 9B). The schematic representation of p38 MAP kinase pathway in *Cln3*$^{\Delta ex7/8}$ mouse brain shows p38 MAPK phosphorylation and thus activation leads to apoptosis (Figure 9C). The effect of flupirtine treatment on the p38 MAP kinase pathway in *Cln3*$^{\Delta ex7/8}$ mouse brain is shown in Figure 9D. It is proposed that flupirtine increases expression of Dusp1 in males and Ppm1d in females to prevent p38 MAPK activation, subsequently preventing apoptosis.

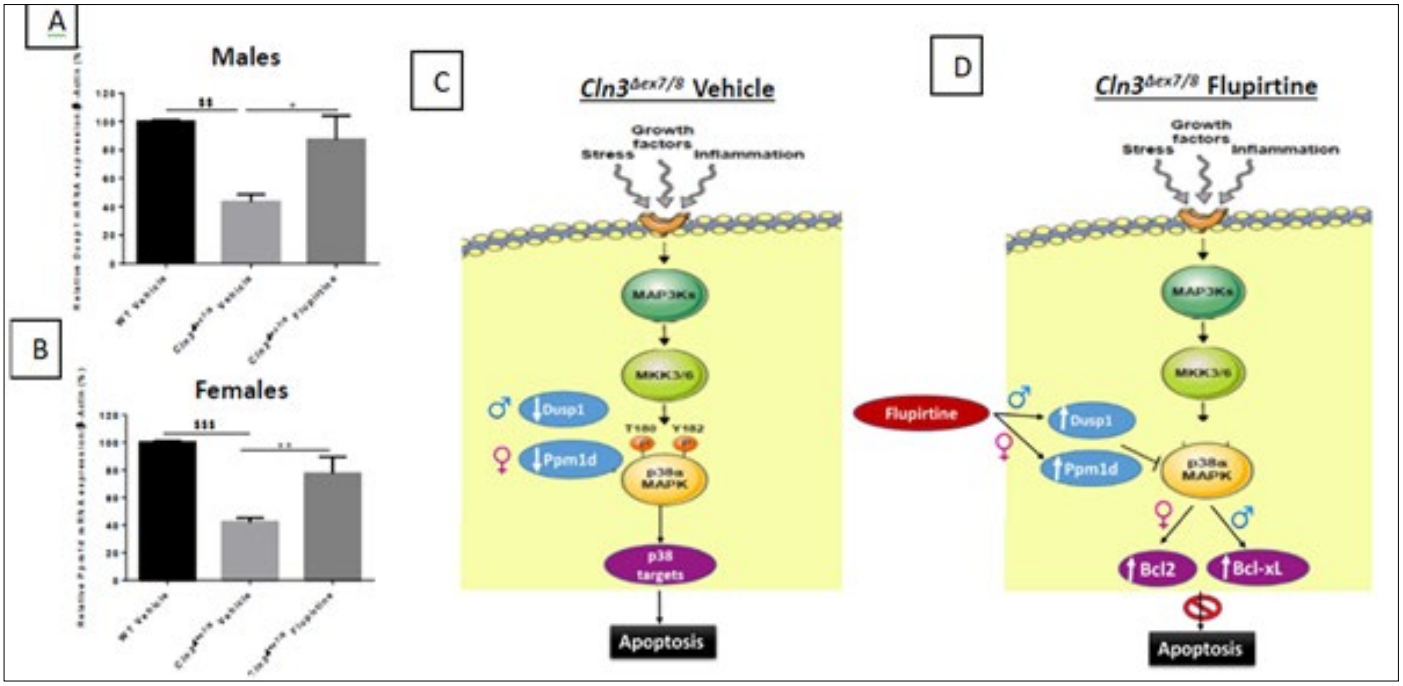

Figure 9: (A) Relative Dusp1 mRNA expression measured by qRT-PCR in WT vehicle-treated, *Cln3Δex7/8* vehicle-treated and *Cln3Δex7/8* flupirtine-treated male mice. (B) Relative Ppm1d mRNA expression measured by qRT-PCR in WT vehicle-treated, *Cln3Δex7/8* vehicle-treated and *Cln3Δex7/8* flupirtine-treated female mice. Data is expressed as mean ± SEM. $p < 0.05 compared to vehicle-treated WT, *p < 0.05 compared to vehicle-treated *Cln3Δex7/8* (*p < 0.05, **p < 0.01, and ***p < 0.001). Schematic representation of (C) p38 MAP kinase pathway in *Cln3Δex7/8* mouse brain, and (D) effect of flupirtine treatment on the p38 MAP kinase pathway in *Cln3Δex7/8* mouse brain.

Table 3: Comparative analysis of DEGs related to p38 MAP Kinase pathway in brain from male and female *Cln3Δex7/8* mice. DEGs related to the p38 MAP Kinase pathway in brain from male and female *Cln3Δex7/8* mice based on gene expression in flupirtine- versus vehicle-treated Cln3Δex7/8 mice. Criteria for differential expression are a p-value < 0.05 and a stringency ≥ ± 1.3-fold change in gene expression.

			Cln3Δex7/8 **Flupirtine** vs. *Cln3Δex7/8* **Vehicle**		*Cln3Δex7/8* **Vehicle** vs. **WT Vehicle**	
Sex	**Gene Symbol**	**Gene Title**	**p-value**	**Fold-Change**	**p-value**	**Fold-Change**
Males	Dusp1	dual specificity phosphatase 1	0.033	1.633	0.148	-1.4
Females	Ppm1d	protein phosphatase 1D magnesium-dependent, delta isoform	0.05	1.419	0.297	-1.142

DISCUSSION

CLN3 disease is an inherited condition due to mutations in the CLN3 gene which cause degeneration of the brain induced by accelerated neuronal apoptosis leading to a progressive loss of cognitive and motor skills. It causes blindness and seizures leading to early death. Currently available treatment regimens are largely supportive, not curative, and do not target underlying mechanisms of disease. Various medications improve seizure control, motor control, sleep difficulties, mood disorders, excessive drooling and digestive problems.

Beneficial effects of flupirtine on apoptosis in CLN3-deficient cells and in *Cln3*$^{\Delta ex7/8}$ mice are documented [4,5] confirming flupirtine enhances motor skills, spatial learning and memory retention in *Cln3*$^{\Delta ex7/8}$ male and female mice. Moreover, flupirtine-treated *Cln3*$^{\Delta ex7/8}$ female mice have a remarkable increase in Bcl-2 expression. In males, flupirtine upregulates Bcl-xl expression. Also, reduced ceramide synthesis in flupirtine-treated male mice and increased degradation of ceramide in female flupirtine-treated mice are confirmed. Flupirtine attenuates astrogliosis in the hippocampus of male and female Cln3Δex7/8 brain. This suggests that flupirtine confers neuroprotection and reduces cell death in brains of *Cln3*$^{\Delta ex7/8}$ male and female mice [5].

Here, the underlying mechanisms of neuroprotection conferred by flupirtine in CLN3 disease is explored by genome array analysis to identify differentially expressed genes in *Cln3*$^{\Delta ex7/8}$ male and female mouse brains. Two complement cascade-related genes (C1qb and C1ra), 3 NF-kB-related genes (Nostrin, Map3k14, and Xiap), and 2 MAPK-related genes (Dusp1 and Ppm1d) are upregulated or downregulated in *Cln3*$^{\Delta ex7/8}$ brains, and, effects reversed by flupirtine. Validation by qRT-PCR of the expression of the 7 genes confirms microarray results of flupirtine-treated *Cln3*$^{\Delta ex7/8}$ and vehicle-treated *Cln3*$^{\Delta ex7/8}$ mice. Most likely, these genes are associated with flupirtine-mediated neuroprotection in CLN3 disease.

Pathway analysis data uncovered several signaling pathways involved in flupirtine-mediated neuroprotection, including the complement cascade, NF-kB and p38α/MAPK signaling pathways. These signaling pathways are closely associated with apoptosis [15-18]. The neuroprotective effect of flupirtine in CLN3 disease is mediated via several signaling pathways and molecules in a complex signal transmission network, albeit, in a gender-specific manner.

The complement cascade is one of the major pathways implicated in flupirtine treatment of both male and female Cln3Δex7/8 mice. In mammals and other higher vertebrates, the complement system, a complex protein network, consists of ≈ 30 plasma proteins involved in lysis, inflammation and clearing opsonized microorganisms [19]. Bacterial infection and/or inflammation lead to upregulation of complement mRNA expression in the central nervous system (CNS) [20]. In fact, neuroinflammation induces reactive gliosis and contributes to ultimate total neuronal loss leading to activation of the complement system in the CNS. Neuroinflammation is described in several central neurodegenerative disorders. Upregulation of inflammatory signaling pathways is well described in Charcot-Marie-Tooth (CMT) neuropathy and amyotrophic lateral sclerosis (ALS) [21]. Complement component 1, q subcomponent B (C1qb) is well established in the literature as a key biomarker for neuroinflammation of a mounted immune response [22]. CMT and ALS patients manifest a prominent increase in C1qb gene expression and protein levels, which drives activation of microglia in disease progression leading to phagocytosis of dying motor neurons [21,23]. Similarly, neuronal apoptosis is accompanied by reactive microglial astrogliosis and increased C1qb levels in CA3 hippocampal region corresponding to neuronal degeneration [24]. Microarray analysis confirmed a 1.473-fold increase in expression of C1qb in brain of male vehicle-treated *Cln3*$^{\Delta ex7/8}$ versus WT mice (Table 1).

A consequence in neurodegenerative disease is retinal degeneration and detachment with induction of Müller cell gliosis and activation of glial fibrillary acidic protein (GFAP) [25]. Retinal degeneration in WT mice involves an increase in Complement component 1, r subcomponent A (C1ra) mRNA levels, indicative of the activation of the innate immune response [25]. Reactive microglia express C1ra as a result of inflammatory molecule secretion, hence, neuroinflammation [26]. In this study, microarray analysis uncovers that expression of C1ra was increased 1.344-fold in female vehicle-treated *Cln3*$^{\Delta ex7/8}$ versus WT female mouse brain (Table 1). Upregulation of C1ra

expression validated by qRT-PCR is also significant (Figure 7B). This upregulation in complement system components C1qb (in male mice) and C1ra (in female mice) could be a consequence of neuronal apoptotic cell death and increased astrogliosis documented in the hippocampus of vehicle-treated *Cln3*$^{\Delta ex7/8}$ mice [5]. Flupirtine treatment significantly lowers gene expression of C1qb and C1ra by 1.3 fold in male and female *Cln3*$^{\Delta ex7/8}$ mice, respectively (Table 1). This highlights the potential of flupirtine in reducing apoptosis and neuroinflammation in brains of Cln3Δex7/8 male and female mice at 18 weeks of age.

Another important signaling pathway implicated in flupirtine-treated *Cln3*$^{\Delta ex7/8}$ mice is the NF-kB signaling pathway. The transcription factor NF-kB regulates immune functions and plays a pivotal role in inflammatory responses and cell survival [27]. X-linked inhibitor of apoptosis protein (Xiap) acts as a strong stimulator of NF-kB through activation of the mitogen-activated protein kinase kinase kinase (MAP3K) signaling pathway [28]. XIAP belongs to the inhibitors of apoptosis (IAP) family of proteins and is considered as the most potent anti-apoptotic protein in vitro. It directly inhibits the caspase cascade [29]. Xiap is upregulated in both male and female *Cln3*$^{\Delta ex7/8}$ mice treated with flupirtine compared to vehicle-treated *Cln3*$^{\Delta ex7/8}$ mice (Table 2) (Figures 8B and 8D). Upstream modulators of XIAP, however, differ between the two sexes. Flupirtine-treated male *Cln3*$^{\Delta ex7/8}$ mice show significantly lower mRNA levels of Nostrin (1.461-fold) compared to male vehicle-treated *Cln3*$^{\Delta ex7/8}$ mice. Flupirtine-treated female

mice show less mRNA levels of Map3k14 (1.319-fold) compared to female vehicle-treated *Cln3*$^{\Delta ex7/8}$ mice (Table 2). Results are validated by qRT-PCR (Figures 8A and 8C).

Nostrin binds to endothelial nitric oxide synthase (eNOS) causing inhibited nitric oxide (NO) production [30]. NO is a gaseous free radical molecule with pleiotropic functions. It regulates synapse plasticity, neurotransmitter release and hormone production, all involved in neurodegenerative diseases [31]. Higher Nostrin expression is present in a pro-inflammatory milieu and an environment with increased oxidative stress and unbalanced cytokines [32]. Flupirtine-treated male *Cln3*$^{\Delta ex7/8}$ mouse brain expressed significantly lower mRNA levels of Nostrin and consequently, higher NO production compared to vehicle-treated *Cln3*$^{\Delta ex7/8}$ male mouse brain (Table 2) (Figure 8A). Higher NO production mediates neuronal cell survival and differentiation, in addition to attenuating apoptotic cell death mechanisms [31], perhaps by lowering ceramide generation [33]. This agrees with significantly decreased level of Sptlc3, a ceramide synthesis enzyme, previously documented in flupirtine-treated male *Cln3*$^{\Delta ex7/8}$ mouse brain compared to vehicle-treated *Cln3*$^{\Delta ex7/8}$ mice [5].

In female *Cln3*$^{\Delta ex7/8}$ brain, mitogen-activated protein kinase kinase kinase 14 (Map3k14) is implicated. MAP3K14 is established as a cell death regulator in cancer cells which is detrimental to neurogenesis [34]. In neurological disorders, activated Map3k14 acts on downstream signaling molecules [35]. NF-kB acts at the crossroads of several signaling pathways. It is regulated by MAPK, requires ubiquitination and proteasomal degradation, chemokine secretion and regulates apoptosis [34]. A robust activation of MAP3K14 is a major phenomenon observed in epilepsy and in experimental models of traumatic brain injury [36]. Other studies claim downregulation of Map3k14 gene expression is related to lowering of cell death and inflammation in vivo [34]. The trend towards lower expression of Map3k14 in brains of flupirtine-treated *Cln3*$^{\Delta ex7/8}$ female mice compared to vehicle-treated *Cln3*$^{\Delta ex7/8}$ mice suggests that findings pinpoint to an enhanced neuroprotective effect of flupirtine in vivo (Table 2) (Figure 8C), hopefully translatable to the clinical setting.

Mitogen-activated protein kinases (MAPKs) constitute a family of conserved enzymes, mainly serine/threonine kinases that act as signal transduction mediators and are involved in cell differentiation, apoptosis, and the cell cycle [37]. The three major signaling cascades involve extracellular signal-regulated kinase 1/2 (ERK1/2), c-Jun N-terminal kinase (JNK), or p38 MAPK [38]. Irregularities in p38 MAPK signaling in neuronal cells are linked to neuroinflammatory processes and diseases such as Alzheimer, Parkinson, amyotrophic lateral sclerosis and Pick disease [39]. Four different p38 MAPK are identified each encoded by a single gene: p38α (MAPK14), p38β (MAPK11), p38γ (MAPK12) and p38δ (MAPK13). The majority of p38 MAPK functions are carried out by p38α [40]. The p38 MAPK enzyme activated by dual phosphorylation of threonine (Thr) and tyrosine (Tyr) by either MAP kinase kinase 3 (MKK3) or MAP kinase kinase 6 (MKK6), is regarded as a stress-induced kinase and plays a critical role in inflammatory responses (Figure 9C). p38 MAPK phosphorylates and activates proteins of the B-cell lymphoma 2 or Bcl-2 family. The latter consists of anti-apoptotic proteins Bcl-2 and Bcl-xL and pro-apoptotic proteins Bax and Bim [41]. The p38 MAPK phosphorylates other targets such as transcription factor p53 that induces expression of death receptors and activates pro-apoptotic members of the Bcl-2 family, increasing apoptosis.

MAPKs can be dephosphorylated by tyrosine-specific phosphatases, serine-threonine phosphatases or dual-specificity (Thr/Tyr) phosphatases (DUSPs). Dual-specificity phosphatase 1 (Dusp1), also known as Mkp-1 (mitogen-activated protein kinase), is one of an 11-member family. It inhibits activity of MAPKs by dephosphorylating tyrosine and threonine residues and is an inhibitor of the p38 MAPK signaling pathway [42]. Reduced Dusp1 expression enhances p38 MAPK phosphorylation. Protein Phosphatase 1 D Magnesium-dependent, delta isoform (Ppm1d), also known as Wip1 (Wild-type p53-induced phosphatase 1), is a phosphatase activated in a p53-dependent manner in response to DNA damage. Ppm1d activation results in negative regulation of p53 function and other tumor suppressor pathways by selective inactivation of p38 MAPK [43]. Thus, deficiency of Ppm1d results in activation of p38 MAPK-dependent signaling pathways. Indeed, Dusp1 in males and Ppm1d in females were

significantly downregulated in *Cln3*$^{\Delta ex7/8}$ vehicle-treated mouse brain compared to WT, leading to activation of the p38 MAPK pathway, contributing to neuronal apoptosis observed in CLN3 disease. Reduced expression of the two p38α MAPK regulators is significantly reversed with flupirtine in diseased mice. These findings correlate microarray analysis (Table 3) and qRT-PCR (Figures 9A and 9B). It is proposed using flupirtine to increase expression of Dusp1 in males and Ppm1d in females to prevent p38 MAPK activation, subsequently preventing apoptosis by upregulating anti-apoptotic proteins, more specifically Bcl-2 in female *Cln3*$^{\Delta ex7/8}$ mice and Bcl-xL in male *Cln3*$^{\Delta ex7/8}$ mice (Figure 9D) [44,45].

CONCLUSION

In conclusion, the data indicate that neuroprotection conferred by flupirtine is mediated via the complement cascade, NF-kB signaling, and the p38α MAPK signaling pathways in male and female *Cln3*$^{\Delta ex7/8}$ mice. C1qb, C1ra, Nostrin, Map3k14, Xiap, Dusp1, and Ppm1d genes are involved in this mechanism. It also consolidates that they are involved in the basic mechanisms of enhanced apoptosis in CLN3 disease. Further functional studies are needed to determine the exact mechanism by which these genes are implicated in CLN3 disease.

Taken together, the data suggests that same signaling pathways are modulated by flupirtine, via different proteins in male versus female *Cln3*$^{\Delta ex7/8}$ mouse brain. This implies sex-specific drug regimens may be warranted for treating neurological diseases, in this instance, CLN3 disease in mouse and man. Many of the observed changes documented in gene expression correlate positively resulting in ameliorated behavior, neuropathology, and biochemical changes with short-term flupirtine administration to *Cln3*$^{\Delta ex7/8}$ male and female mice. The findings uncovered lay the foundation for use of neuroprotective flupirtine as a promising drug for treatment of human CLN3 disease.

REFERENCES

1. Dhar S, Bitting RL, Rylova SN, Jansen PJ, Lockhart E, Koeberl DD, et al. Flupirtine blocks apoptosis in batten patient lymphoblasts and in human postmitotic CLN3- and CLN2-deficient neurons. Annals of Neurology. 2002;51(4):448-66.
2. Lane SC, Jolly RD, Schmechel DE, Alroy J, Boustany RM. Apoptosis as the Mechanism of Neurodegeneration in Batten's Disease. Journal of Neurochemistry. 1996;67(2):677-83.
3. Puranam KL, Guo WX, Qian WH, Nikbakht K, Boustany RM. CLN3 Defines a Novel Antiapoptotic Pathway Operative in Neurodegeneration and Mediated by Ceramide. Molecular Genetics and Metabolism. 1999;66(4):294-308.
4. Makoukji J, Saadeh F, Mansour KA, El-Sitt S, Al Ali J, Kinarivala N, et al. Flupirtine derivatives as potential treatment for the neuronal ceroid lipofuscinoses. Annals of Clin and Trans Neuro. 2018;5(9):1089-103.
5. Maalouf K, Makoukji J, Saab S, Makhoul NJ, Carmona AV, Kinarivala N, et al. Exogenous Flupirtine as Potential Treatment for CLN3 Disease. 2020;9(8):1872.
6. Cotman SL, Vrbanac V, Lebel LA, Lee RL, Johnson KA, Donahue LR, et al. Cln3(Deltaex7/8) knock-in mice with the common JNCL mutation exhibit progressive neurologic disease that begins before birth. Hum Mol Genet. 2002;11(22):2709-21.
7. Patil AM, Matter AB, Raol HY, Bourne WAD, Kelley AR, Kompella BU. Brain distribution and metabolism of flupirtine, a nonopioid analgesic drug with antiseizure effects, in neonatal rats. Pharmaceutics. 2018;10(4).
8. Perovic S, Pergande G, Ushijima H, Kelve M, Forrest J, Müller WE. Flupirtine partially prevents neuronal injury induced by prion protein fragment and lead acetate. Neurodegeneration. 1995;4(4):369-74.
9. Müller WEG, Laplanche J-L, Ushijima H, Schröder HC. Novel approaches in diagnosis and therapy of Creutzfeldt–Jakob disease. Mechanisms of Ageing and Development. 2000;116(2):193-218.
10. Huang P, Li C, Fu T, Zhao D, Yi Z, Lu Q, et al. Flupirtine attenuates chronic restraint stress-induced cognitive deficits and hippocampal apoptosis in male mice. Behav Brain Res. 2015;288:1-10.
11. Dhar S, Bitting RL, Rylova SN, Jansen PJ, Lockhart E, Koeberl DD, et al. Flupirtine blocks apoptosis in batten patient lymphoblasts and in human postmitotic CLN3- and CLN2-deficient neurons. Ann Neurol. 2002;51(4):448-66.
12. Kinarivala N, Patel R, Boustany RM, Al-Ahmad A, Trippier PC. Discovery of aromatic carbamates that confer neuroprotective activity by enhancing autophagy and inducing the anti-apoptotic protein b-cell lymphoma 2 (Bcl-2). J Med Chem. 2017;60(23):9739-56.
13. Makoukji J, El-Sitt S, Makhoul NJ, Soueid J, Kadara H, Boustany RM. Sex differences in gene expression with galactosylceramide treatment in *Cln3*$^{\Delta ex7/8}$ mice. PLoS One. 2020;15(10):e0239537.
14. Djordjevic J, Roy Chowdhury S, Snow WM, Perez C, Cadonic C, Fernyhough P, et al. Early onset of sex-dependent mitochondrial deficits in the cortex of 3xtg alzheimer's mice. Cells. 2020;9(6).
15. Boudhabhay I, Poillerat V, Grunenwald A, Torset C, Leon J, Daugan MV, et al. Complement activation is a crucial driver of acute kidney injury in rhabdomyolysis. Kidney Int. 2020.
16. Wang F, Zhang H, Wang C. MiR-590-3p regulates cardiomyocyte P19CL6 proliferation, apoptosis and differentiation in vitro by targeting PTPN1 via JNK/STAT/NF-kB pathway. Int J Exp Pathol. 2020.
17. Sheng X, Qiu C, Liu H, Gluck C, Hsu JY, He J, et al. Systematic integrated analysis of genetic and epigenetic variation in diabetic kidney disease. Proceedings of the

National Academy of Sciences. 2020; 117(46):29013-29024.

18. Zhang T, Pan L, Cao Y, Liu N, Wei W, Li H. Identifying the mechanisms and molecular targets of yizhiqingxin formula on alzheimer's disease: Coupling network pharmacology with geo database. Pharmgenomics Pers Med. 2020;13:487-502.
19. Lu J, Kishore U. C1 Complex: An adaptable proteolytic module for complement and non-complement functions. Frontiers in Immunology. 2017;8(592).
20. van Beek J, Elward K, Gasque P. Activation of complement in the central nervous system: Roles in neurodegeneration and neuroprotection. Ann N Y Acad Sci. 2003;992:56-71.
21. Fernandez-Lizarbe S, Civera-Tregón A, Cantarero L, Herrer I, Juarez P, Hoenicka J, et al. Neuroinflammation in the pathogenesis of axonal Charcot-Marie-Tooth disease caused by lack of GDAP1. Exp Neurol. 2019;320:113004.
22. Vlasova-St Louis I, Chang CC, Shahid S, French MA, Bohjanen PR. transcriptomic predictors of paradoxical cryptococcosis-associated immune reconstitution inflammatory syndrome. Open Forum Infect Dis. 2018;5(7):157.
23. Lee JD, Levin SC, Willis EF, Li R, Woodruff TM, Noakes PG. Complement components are upregulated and correlate with disease progression in the TDP-43Q331K mouse model of amyotrophic lateral sclerosis. J Neuroinfla. 2018;15(1):171.
24. Kraft AD, McPherson CA, Harry GJ. Association Between microglia, inflammatory factors, and complement with loss of hippocampal mossy fiber synapses induced by trimethyltin. Neurotox Res. 2016;30(1):53-66.
25. Augustine J, Pavlou S, Ali I, Harkin K, Ozaki E, Campbell M, et al. IL-33 deficiency causes persistent inflammation and severe neurodegeneration in retinal detachment. J Neuroinflam. 2019;16(1):251.
26. DePaula-Silva AB, Gorbea C, Doty DJ, Libbey JE, Sanchez JMS, Hanak TJ, et al. Differential transcriptional profiles identify microglial- and macrophage-specific gene markers expressed during virus-induced neuroinflammation. J Neuroinflam. 2019;16(1):152.
27. Liu T, Zhang L, Joo D, Sun SC. NF-kB signaling in inflammation. Signal Transduct Target Ther. 2017;2:17023-.
28. Hofer-Warbinek R, Schmid JA, Stehlik C, Binder BR, Lipp J, de Martin R. Activation of NF-kappa B by XIAP, the X chromosome-linked inhibitor of apoptosis, in endothelial cells involves TAK1. J Biol Chem. 2000;275(29):22064-8.
29. Zhao C, Zhao Q, Zhang C, Wang G, Yao Y, Huang X, et al. miR-15b-5p resensitizes colon cancer cells to 5-fluorouracil by promoting apoptosis via the NF-kB/XIAP axis. Scientific Reports.
30. Chakraborty S, Islam S, Saha S, Ain R. Dexamethasone-induced Intra-Uterine Growth Restriction impacts NOSTRIN and its downstream effector genes in the rat mesometrial uterus. Scientific reports. 2018;8(1):8342-.
31. Garthwaite J. Concepts of neural nitric oxide-mediated transmission. Eur J Neurosci. 2008;27(11):2783-802.
32. Mookerjee RP, Wiesenthal A, Icking A, Hodges SJ, Davies NA, Schilling K, et al. Increased gene and protein expression of the novel eNOS regulatory protein NOSTRIN and a variant in alcoholic hepatitis. Gastroenterology. 2007;132(7):2533-41.
33. Sciorati C, Rovere P, Ferrarini M, Heltai S, Manfredi AA, Clementi E. Autocrine nitric oxide modulates CD95-induced apoptosis in gammadelta T lymphocytes. J Biol Chem. 1997;272(37):23211-5.
34. Ortiz A, Husi H, Gonzalez-Lafuente L, Valiño-Rivas L, Fresno M, Sanz AB, et al. Mitogen-activated protein kinase 14 promotes AKI. J Am Soc Nephrol. 2017;28(3):823-36.
35. Borsini A, Stangl D, Jeffries AR, Pariante CM, Thuret S. The role of omega-3 fatty acids in preventing glucocorticoid-induced reduction in human hippocampal neurogenesis and increase in apoptosis. Translational Psychiatry. 2020;10(1):219.
36. Srivastava PK, Roncon P, Lukasiuk K, Gorter JA, Aronica E, Pitkänen A, et al. Meta-Analysis of micrornas dysregulated in the hippocampal dentate gyrus of animal models of epilepsy. eNeuro. 2017;4(6).
37. Corrêa SAL, Eales KL. The Role of p38 MAPK and Its substrates in neuronal plasticity and neurodegenerative disease. J Signal Transduc. 2012;2012:649079.
38. Plotnikov A, Zehorai E, Procaccia S, Seger R. The MAPK cascades: Signaling components, nuclear roles and mechanisms of nuclear translocation. Biochim Biophys Acta. 2011;1813(9):1619-33.
39. Harper SJ, LoGrasso P. Signalling for survival and death in neurones: The role of stress-activated kinases, JNK and p38. Cell Signal. 2001;13(5):299-310.
40. Cuadrado A, Nebreda AR. Mechanisms and functions of p38 MAPK signalling. Biochem J. 2010;429(3):403-17.
41. Gräb J, Rybniker J. The Expanding role of p38 mitogen-activated protein kinase in programmed host cell death. Microbiology Insights. 2019;12:1178.
42. Zhao Q, Shepherd EG, Manson ME, Nelin LD, Sorokin A, Liu Y. The role of mitogen-activated protein kinase phosphatase-1 in the response of alveolar macrophages to lipopolysaccharide: Attenuation of proinflammatory cytokine biosynthesis via feedback control of p38. J Biol Chem. 2005;280(9):8101-8.
43. Bulavin DV, Phillips C, Nannenga B, Timofeev O, Donehower LA, Anderson CW, et al. Inactivation of the Wip1 phosphatase inhibits mammary tumorigenesis through p38 MAPK-mediated activation of the p16(Ink4a)-p19(Arf) pathway. Nat Genet. 2004;36(4):343-50.

44. Morecroft I, Murray A, Nilsen M, Gurney AM, MacLean MR. Treatment with the Kv7 potassium channel activator flupirtine is beneficial in two independent mouse models of pulmonary hypertension. Br J Pharmacol. 2009;157(7):1241-9.

45. Irizarry RA, Hobbs B, Collin F, Beazer□Barclay YD, Antonellis KJ, Scherf U, et al. Exploration, normalization, and summaries of high density oligonucleotide array probe level data. Biostatistics. 2003;4(2):249-64.